Lysyl oxidase-like 2 is highly expressed in colorectal cancer cells and promotes the development of colorectal cancer

XIMAO CUI[1,2*], GUANGHUI WANG[1-3*], WENBIN SHEN[1,2], ZHENYU HUANG[1,2], HAILAN HE[1,2] and LONG CUI[1,2]

[1]Department of Colorectal and Anal Surgery, Xinhua Hospital, Shanghai Jiao Tong University School of Medicine, Shanghai 200092; [2]Shanghai Colorectal Cancer Research Center, Shanghai 200092; [3]Department of Gastrointestinal Surgery, Guizhou Provincial People's Hospital, Guiyang, Guizhou 550002, P.R. China

Received December 18, 2017; Accepted May 17, 2018

DOI: 10.3892/or.2018.6452

Abstract. Colorectal cancer (CRC) is the third most common type of cancer. In the present study, the expression and intracellular localization of lysyl oxidase-like 2 (LOXL2) protein in CRC were examined. Quantitative polymerase chain reaction and western blot analysis of LOXL2 mRNA and protein expression was performed for 40 pairs of CRC tumor and normal mucosa tissue samples. The immunohistochemical staining of tissue microarrays was performed to detect LOXL2 protein expression. LOXL2 was highly expressed in the extracellular matrix and CRC cells. The positive expression of LOXL2 in CRC cells was significantly associated with the tumor tumor-node metastasis stage and distant metastasis, while elevated LOXL2 expression within the CRC cells was an independent prognostic factor in patients with CRC. The knockdown of LOXL2 impaired the proliferative and migratory abilities of CRC cells *in vitro* and *in vivo*, and induced cell cycle arrest and apoptosis. These findings indicated that LOXL2 might have an important role in CRC.

Introduction

Colorectal cancer (CRC) is the third most common type of cancer, comprising 9.7% of all cancer cases, and the fourth most common cause of mortalities due to cancer globally (8.5% of all cancer mortalities), accounting for ~1.4 million new cases and 697,000 mortalities per year (1). The incidence of CRC increases with age; the median age at the time of diagnosis for CRC is 68 for men and 72 for women (2). The 5-year survival rate for CRC ranges from 50% in developing countries to 65% in developed countries (3). The treatment of CRC depends on the location of the tumor and the disease stage at diagnosis. For early-stage CRC, surgery alone can eliminate cancer (4). For late-stage CRC, chemotherapy is used alone or in combination with radiotherapy to treat metastases (5). The metastasis of CRC is a critical indicator of survival rate. The 5-year survival rate is >90% if CRC is diagnosed at an early stage (6). If the tumor has spread to the adjacent lymph nodes, the 5-year survival rate is <70%. Nevertheless, if the tumor has metastasized to distant organs, the 5-year survival rate is 11.7% (2). The clinical outcome for patients with CRC is far from satisfactory, particularly for patients with advanced cancer (stage III or IV). Therefore, the identification of molecular markers for tumor progression and metastasis, which may also be targets for therapeutic intervention, is urgently required for personalized and accurate treatment and diagnosis.

Lysyl oxidase-like 2 (LOXL2) is a member of the lysyl oxidase family of proteins, which includes lysine oxidase (LOX) and four lysyl oxidase-like proteins (LOXLl, LOXL2, LOXL3 and LOXL4) (7). The LOX family is crucial for the formation of connective tissues. The proteins in the LOX family of are extracellular copper-dependent amine oxidases that catalyze the first step in the formation of collagen-elastin crosslinks. Numerous studies have implicated LOXL2 in fibrotic diseases (8,9). A number of studies have also demonstrated an association between LOXL2 and cancer progression. LOXL2 is upregulated in many types of cancer and is associated with a poor outcome (10). LOXL2 expression is also positively associated with cancer metastasis due to its role in the formation of covalent collagen-elastin crosslinks in the extracellular matrix (ECM) (11-14).

In a previous study by the authors, the differences in the mRNA expression profile for 8 CRC tumor samples compared with paired normal mucosa were determined using microarray analysis (15). LOXL2 expression was upregulated in the CRC tissue samples compared with the paired normal tissues. In the present study, the intracellular expression of LOXL2 protein in CRC tissues compared with corresponding normal tissues was examined, and the potential associations with the disease clinicopathological features and prognosis were analyzed. The

Correspondence to: Professor Long Cui, Department of Colorectal and Anal Surgery, Xinhua Hospital, Shanghai Jiao Tong University School of Medicine, 1665 Kongjiang Road, Shanghai 200092, P.R. China
E-mail: cuilong@xinhuamed.com.cn

*Contributed equally

Key words: colorectal cancer, LOXL2, prognosis, proliferation, migration

mechanism of action for the effect of LOXL2 in CRC cell lines was also evaluated.

Materials and methods

Collection of CRC specimens. A total of 228 human CRC and matched normal samples were collected by biopsy from the Department of Colorectal Surgery, Xinhua Hospital, Shanghai Jiaotong University School of Medicine (Shanghai, China). Informed consent was obtained for the collection of all specimens, and the present study was approved by the institutional review board. These experiments were conducted in accordance with the ethical standards of the Helsinki Declaration of 1964 and its subsequent amendments or comparable ethical standards. A total of 40 CRC samples were analyzed by reverse transcription-quantitative polymerase chain reaction (RT-qPCR). Tissue microarrays were prepared from 228 CRC specimens and subjected to immunohistochemical analysis.

Cell culture. A total of 6 human CRC cell lines, including SW480, SW620, HT29, HCT116, DLD1 and LOVO cells, and 293T cells for luciferase reporter assays, were cultured in Dulbecco's modified Eagle's medium (Corning Life Sciences, Tewksbury, MA, USA) with 10% fetal bovine serum (Gibco; Thermo Fisher Scientific, Inc., Waltham, MA, USA). The cells were cultured in a 5% CO_2 humidified atmosphere at 37˚C and passaged every 3-4 days.

RNA isolation and RT-qPCR. Total RNA was extracted with RNAiso (Takara Biotechnology Co., Ltd., Dalian, China), and the PrimeScript® RT-PCR kit (Takara Biotechnology Co., Ltd.) was used to generate cDNA. qPCR was performed using an ABI 7500 cycler (Thermo Fisher Scientific, Inc.) and SYBR® Premix Ex Taq™ (Takara Biotechnology Co., Ltd.). ACTB served as an internal control. The primers used are as follows: LOXL2-F, 5'-CCTGTCTTCGGGCTGATG-3' and LOXL2-R, 5'-CACTGCGGATCCCTGAAAC-3'; ACTB-F, 5'-GTTGTCGACGACGAGCG-3' and ACTB-R, 5'-GCACAGAGCCTCGCCTT-3'. The Thermal Cycler Dice system (Takara Biotechnology Co., Ltd.) was used for qPCR with the following conditions: 95˚C for 5 min, 50 cycles of 95˚C for 5 sec and 60˚C for 10 sec. Each value was normalized to the levels of ACTB. The PCR reaction was performed in triplicate, and the relative gene expression was analyzed by the $2^{-\Delta\Delta Cq}$ method (16).

Immunohistochemistry. The paraffin sections were deparaffinized, rehydrated and treated according to the standard protocol. Following incubation with a monoclonal anti-human LOXL2 antibody (dilution, 1:1,000; catalog no., ab179810, Abcam, Cambridge, MA, UK) or phosphate-buffered saline (PBS; negative control) overnight, the sections were washed three times with PBS and incubated with a horseradish peroxidase-labeled secondary antibody (dilution, 1:1,000; catalog no., GK500710; Gene Company Ltd., Shanghai, China) for 30 min at room temperature. The sections were stained with 3',3-diaminobenzidine solution after washing in PBS. The sections were then counterstained with 0.1% hematoxylin and sealed with coverslips. LOXL2 staining was graded according to staining intensity and staining rate. The criteria for staining intensity are as follows: 0, no staining; 1, mild staining; 2, moderate staining or 3, strongly positive. The criteria for staining rate are as follows: 1, 0-25% positive cells; 2, 26-50%; 3, 51-75% or 4, >75%, as previously described (17). For each section, a semi-quantitative score was calculated by multiplying these two values (from 0 to 12). A total of 2 histopathologists blinded to the clinical data were assigned to review and score the slides.

Immunoblotting. Immunoblotting was performed as previously described (18). The proteins were separated by 10% SDS-PAGE polyacrylamide gel electrophoresis and transferred to a nitrocellulose membrane. The membranes were blocked with 5% skimmed milk in PBS buffer for 1 h at room temperature then incubated overnight at 4˚C with the primary antibodies, including anti-LOXL2 (dilution, 1:500; catalog no., ab179810, Abcam); anti-vimentin (dilution, 1:1,000; catalog no., ab92547, Abcam); anti-CCNE1 (dilution, 1:1000; catalog no., sc-377100, Santa Cruz Biotechnology, Inc., Dallas, TX, USA); anti-CDK2 (cyclin dependent kinase 2; dilution, 1:1,000; catalog no., 2546, Cell Signaling Technology, Inc., Danvers, MA, USA); anti-cleaved poly(ADP-ribose) polymerase (PARP; dilution, 1:5,000; catalog no., ab32064, Abcam); and anti-ACTB (dilution, 1:20,000; catalog no., A3854, Sigma-Aldrich; Merck KGaA, Darmstadt, Germany). After washing with TBST for 3 times (10 min for each wash), the membranes were incubated with a horseradish peroxidase-labeled secondary antibody (HRP-labeled goat anti-rabbit IgG (H+L), catalog no., A0208 or HRP-labeled goat anti-mouse IgG (H+L), catalog no., A0216, dilution, 1:1,000; Beyotime Institute of Biotechnology, Haimen, China) for 1 h at room temperature and then visualized with a chemiluminescence reagent (EMD Millipore, Billerica, MA, USA).

RNA interference. For the shRNA-mediated knockdown of LOXL2 induced by doxycycline (DOX), oligonucleotides encoding LOXL2 targeting shRNAs and their complement were synthesized, including LOXL2-sh1, 5'-CCGGACA ATACCAAAGTGTACAACTCGAGTTGTACACTTTGGTA TTGTTTTTTG-3' and LOXL2-sh2, 5'-CCGGCGATTAC TCCAACAACATCATCTCGAGATGATGTTGTTGGAGTA ATCGTTTTTG-3'. The sequence published by Sigma-Aldrich (Merck KGaA) was referred to. After transfection for 8 h in 293T cells (American Type Culture Collection, Manassas, VA, USA), the cell culture medium was changed to normal DMEM high glucose medium containing fetal bovine serum and penicillin-streptomycin. Viral particles were harvested after 48 h of transfection. HCT116 and DLD1 were incubated with viral particles for 8 h. The viral titer was determined by positive count of green fluorescent protein. The cells that were not infected would be killed by puromycin. The 4 pmol oligonucleotide sense and antisense pairs were inserted into the lentiviral expression system, pLKO-TET-ON vector (20 ng; Addgene, Inc., Cambridge, MA, USA) (19). The cells stably expressing shRNA induced by DOX were cultured in puromycin-containing (1 μg/ml) medium. The cells cultured without DOX were used for control. The incubation of the cells for 48 h at 37˚C with 500 ng/ml DOX induced the knockdown of LOXL2.

Cell proliferation assay. Cell growth was measured using a Cell Counting Kit-8 (CCK-8 kit; Dojindo Molecular Technologies, Inc., Kumamoto, Japan), which detects the dehydrogenase activity of the viable cells. Briefly, the cells ($2x10^3$/well) were seeded in 96-well plates of 5 repeats and incubated for 24 h at 37˚C. The cells cultured without DOX were used for control. The incubation of the cells for 48 h at 37˚C with 500 ng/ml DOX induced the knockdown of LOXL2. CCK-8 solution (10 μl) was added to each well and incubated at 37˚C for a further 1 h in an incubator. The absorbance at 450 nm was measured using a microplate reader. In addition, a colony formation assay was performed. A total of $1x10^3$ cells were seeded in 6-well plates and incubated at 37˚C for 2 weeks. After incubation, the cells were fixed with 100% methanol and stained with 0.1% crystal violet for 10 min at room temperature. The cells were observed under an inverted microscope, and images were captured in a vertical field of view. The experiment was performed in triplicate.

Cell cycle analysis. The cells were treated with 70% ice-cold ethanol overnight. The cells were treated with propidium iodide (PI; 20 μg/ml, catalog no., 550825; BD Biosciences, San Jose, CA, USA) at 4˚C in the dark for 30 min. A flow cytometer (Beckman Coulter, Inc., Brea, CA, USA) was used for analyzing the DNA content for cell cycle analysis. The software CytExpert (version no., 1.2.11.0, Beckman Coulter, Inc., Suzhou, Jiangsu, China) was used for anlaysis. The experiment was performed in triplicate.

Detection of apoptosis. The detection of the rate of apoptosis was performed using an FITC Annexin V Apoptosis Detection kit (BD Pharmingen; BD Biosciences). The cells were trypsinized, washed in PBS and resuspended in 1X binding buffer at a density of 10^6 cells/ml. A total of 100 μl of the suspension was transferred to a 5 ml culture tube. FITC-Annexin V (5 μl) and PI (5 μl) were added to the tube. The samples were vortexed for 15 min at 25˚C in the dark. After incubation, 400 μl 1X binding buffer was added to each tube. The rate of apoptosis was determined by CytExpert (version no., 1.2.11.0, Beckman Coulter, Inc., Suzhou, Jiangsu, China) using flow cytometry (Beckman Coulter, Inc.) within 1 h.

Wound-healing assay, Transwell and luciferase assays. For the wound-healing assays, the cells (10^6) were cultured in complete medium [Dulbecco's modified Eagle's medium (Corning Life Sciences) with 10% fetal bovine serum (Gibco; Thermo Fisher Scientific, Inc.)] and seeded in 6-well plates. After 8 h, the medium was changed to a low-serum medium (Dulbecco's modified Eagle's medium with 1% fetal bovine serum). A wound was produced in the cell monolayer, and the cells were cultured for an additional 72 h at 37˚C. Images were acquired immediately after wound scratching and at 72 h. For Transwell assay, the cells (10^5) were seeded in a growth factor-deficient upper chamber. Complete medium was added to the lower chamber. Cell migration was analyzed after 48 h as previously described (20). Luciferase assays were performed as previously described (21). Briefly, 200 ng vimentin-Luc reporter plasmid was co-transfected with pGL3 basic plasmid (200 ng) or pGL3-LOXL2 plasmid (200 ng) into 293T cells along with *Renilla* luciferase plasmid (20 ng; Promega, Madison, WI, USA).

Xenograft tumor formation and lung metastasis mouse model. A total of 10 male nude mice (4-6 weeks old; weight, ~20 g) were obtained from SLAC Lab Animal (Shanghai SLAC Laboratory Animal Co., Ltd., Shanghai, China). The animal care and use committees of Xinhua Hospital approved all mouse procedures. To establish xenograft tumors, shLOXL2 TET-ON DLD1 cells (10^6) were subcutaneously injected into both axillary fat pads. The mice were randomized into two groups (5 mice/group) and received either normal water (control group) or water containing 1 mg/ml DOX for 4 weeks. Water was renewed every other day. The growth of the tumors was measured 4 weeks later by sacrificing the mice and determining the weight of the tumors. To establish a lung metastasis model, DLD1 cells (10^6) were injected into the tail veins of 12 mice (n=6 per group), which then received the same treatments as described above. After 8 weeks, the mice were sacrificed, and both lungs were resected and imaged. The lung tissue sections were stained with hematoxylin and eosin for 5 min at room temperature, and lung metastases were observed under a microscope by a pathologist who was blinded to the treatment status of the mice. The animal experiments were approved by the Xinhua hospital review board.

Statistical analysis. Statistical analysis was performed using SPSS software (version 18; SPSS, Inc., Chicago, IL, USA). Student's t-test was used to compare continuous variables. Pearson's χ^2 test was used to assess the association between the expression of LOXL2 and clinicopathological parameters. Survival curves were drawn using the Kaplan-Meier method and compared using the log-rank test. Univariate and multivariate analyses were performed using the Cox proportional hazards regression model. A two-tailed P-value of 0.05 was considered statistically significant.

Results

Upregulation of LOXL2 in CRC cells and its prognostic value for patients with CRC. LOXL2 was identified as an upregulated gene in CRC by a mRNA microarray in a previous study by the authors (P<0.0001; Fig. 1A) (15). Therefore, in the present study, the microarray results were validated. RT-qPCR was performed to detect the level of LOXL2 mRNA expression in 40 paired CRC and normal adjacent tissues. The level of LOXL2 mRNA expression was significantly elevated in CRC tissues compared with normal tissues (P<0.0001; Fig. 1B). Western blot analysis was performed on 7 paired CRC and normal adjacent tissues, and observed that the level of LOXL2 protein was also elevated in CRC tissues compared with normal colorectal tissues (Fig. 1C).

Immunohistochemistry was next performed in 228 CRC tissues and adjacent normal colon tissues. Representative images are shown in Fig. 1E. Low LOXL2 expression was detected in the epithelial cells of normal tissues (Fig. 1Ea), while a low to high LOXL2 expression was identified in the epithelial cells of tumor tissues (Fig. 1Eb and c). LOXL2 expression was observed not only in the ECM but also in the CRC cells. Notably, in a considerable number of LOXL2-positive

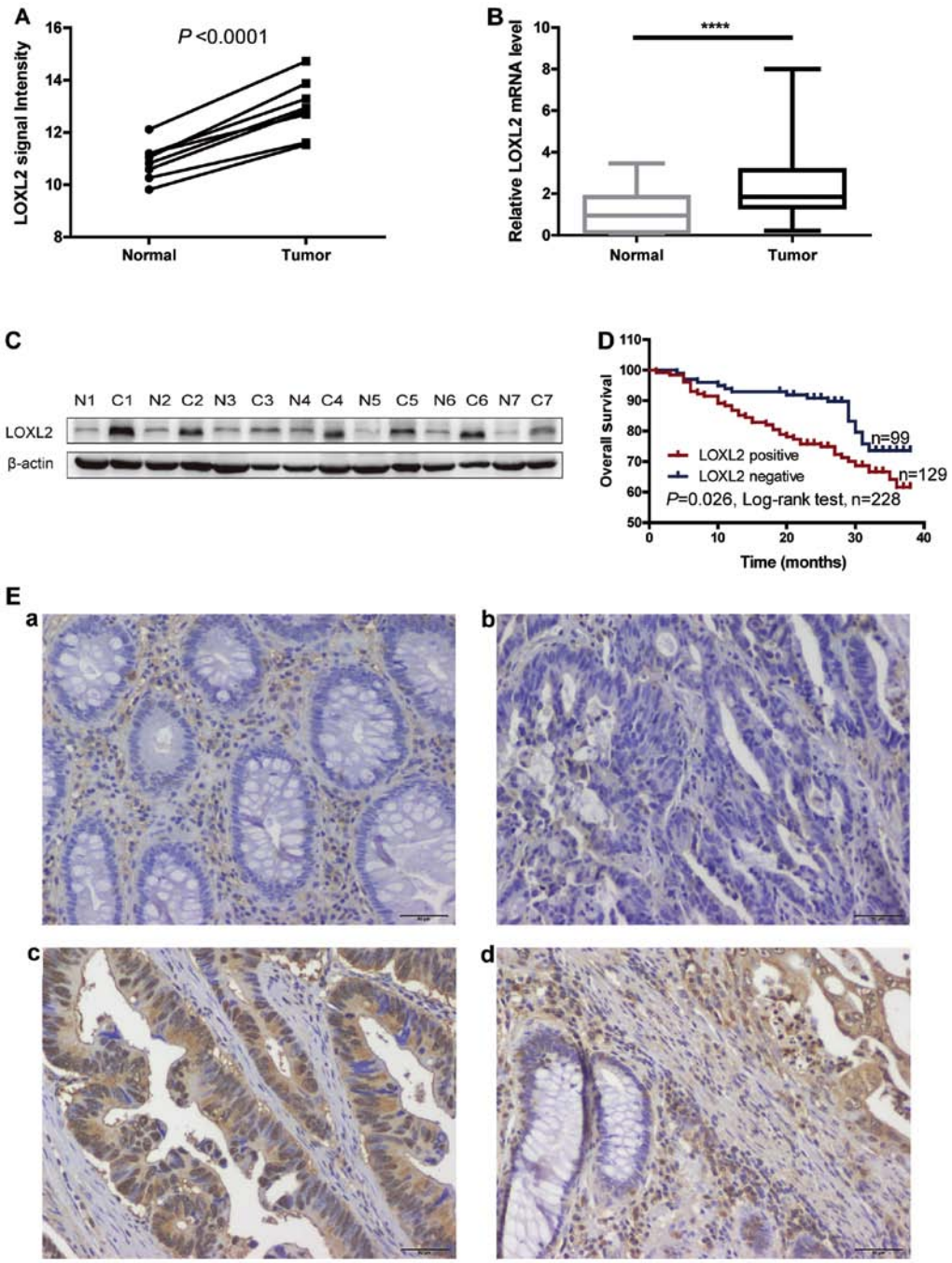

Figure 1. Elevated expression of LOXL2 in CRC. (A) An mRNA microarray, demonstrating the upregulation of LOXL2 in 8 CRC tissue samples compared with paired normal colorectal mucosa. (B) Reverse transcription quantitative-polymerase chain reaction detection of LOXL2 expression in 40 CRC tumor tissue samples and corresponding normal mucosa. ****P<0.0001. (C) Western blot analysis of LOXL2 protein in 7 CRC samples (C1-7) compared with normal colorectal mucosa (N1-7). ACTB was used as a loading control. (D) The Kaplan-Meier plots were stratified by LOXL2 expression for overall survival in patients with CRC. Statistical significance was determined by a log-rank test. (E) Immunohistochemical analysis of LOXL2 in CRC and normal mucosa tissue samples. Representative images of (a) normal mucosa tissue; (b) CRC tissues with a low level of LOXL2 expression; (c) CRC tissues with a high level of LOXL2 expression and (d) LOXL2 expression in CRC cells in the invasive margin. Magnification, x200. Scale bar, 50 μm. LOXL2, Lysyl oxidase-like 2; CRC, colorectal cancer.

cells, LOXL2 was localized to the cell nucleus (Fig. 1Ec). The expression pattern of LOXL2 was different between normal and CRC tissues (Fig. 1Ed). The positive expression ratio for LOXL2 in epithelial cells was 56.6% (129/228) in CRC tissues and 7.89% (18/228) in normal tissues.

The association between LOXL2 protein expression and pathological features, including sex, age, tumor size, T, N and M classifications, tumor-node metastasis (TNM) stage and tumor differentiation, were analyzed in patients with CRC (Table I). The analysis revealed that a high LOXL2 protein expression was associated with TNM stage (P=0.001), N classification (P=0.006) and M classification (P=0.032), but there was no significant association with age, sex, tumor diameter, T classification or differentiation.

Next, the Kaplan-Meier method was used to investigate the significance of tumor LOXL2 expression in survival

Table I. Association of LOXL2 epithelial/tumor cell staining with the pathological and clinical features of patients with colorectal cancer.

Variables	All cases (n=228)	LOXL2 epithelial/tumor cell staining: Absent, n (%) (n=100)	LOXL2 epithelial/tumor cell staining: Positive, n (%) (n=128)	P-values
Age, years[c]				0.930[a]
≤63	119	52 (43.7)	67 (56.3)	
>63	109	47 (43.1)	62 (56.9)	
Sex				0.978[a]
Male	108	47 (43.5)	61 (56.5)	
Female	120	52 (43.3)	68 (56.7)	
Tumor size (cm)				0.230[a]
≤5 cm	98	47 (48.0)	51 (52.0)	
>5 cm	130	52 (40.0)	78 (60.0)	
TNM stage				<0.001[b]
I	42	30 (71.4)	12 (28.6)	
II	69	29 (42.0)	40 (58.0)	
III	75	28 (37.3)	47 (62.7)	
IV	42	12 (28.6)	30 (71.4)	
T stage				0.188[b]
I	4	2 (50.0)	2 (50.0)	
II	53	28 (52.8)	25 (47.2)	
III	66	22 (33.3)	44 (66.7)	
IV	105	47 (44.8)	58 (55.2)	
Lymphatic metastasis				0.006[b]
N_0	117	61 (52.1)	56 (47.9)	
N_1	65	18 (27.7)	47 (72.3)	
N_2	46	20 (43.5)	26 (56.5)	
Distal metastasis				0.032[a]
M_0	186	87 (46.8)	99 (53.2)	
M_1	42	12 (28.6)	30 (71.4)	
Differentiation				0.623[b]
Well	31	15 (48.4)	16 (51.6)	
Moderate	190	82 (43.2)	108 (56.8)	
Poor	7	2 (28.6)	5 (71.4)	

[a]Mann-Whitney U-test; [b]Spearman test; [c]median age at operation; LOXL2, lysyl oxidase-like 2; TNM, tumor-node metastasis.

prognosis. As indicated in Fig. 1D, log-rank tests revealed that LOXL2 expression was significantly associated with shortened patient survival time (P=0.026). In addition, univariate and multivariate Cox regression hazard analyses indicated that LOXL2 expression was an independent prognostic indicator for CRC (Table II). These data indicated that LOXL2 might be an appropriate marker for predicting the prognosis of patients with CRC.

LOXL2 knockdown impairs the proliferation of CRC cells in vitro. To further determine the expression of LOXL2 in CRC epithelial cells, LOXL2 mRNA and protein levels were examined in 6 CRC cell lines (Fig. 2A and B). Among the 6 cell lines, HCT116 and DLD1 cells expressed relatively higher levels of LOXL2 mRNA and protein, and were therefore selected for further analysis. To examine the function of LOXL2, LOXL2 knockdown cells were generated by infecting HCT116 and DLD1 with two TET-ON pLKO lentiviruses that encode LOXL2-targeting shRNAs (shRNA1 and shRNA2). Stable lines were selected, and the LOXL2 knockdown efficiency after 48 h of DOX treatment was confirmed by qPCR and immunoblotting (Fig. 2C-E).

The effects of LOXL2 knockdown (shRNA2) in the stable cell lines on cell proliferation were evaluated using CCK8 assays. It was indicated that the knockdown of LOXL2 in HCT116 and DLD1 cells significantly decreased the growth

Table II. Univariate and multivariable OS analyses for LOXL2 expression in CRC cells in patients with CRC.

	OS		
Parameters	HR (95% CI)	P-value	*n* (events)
Univariate			
Negative LOXL2 staining	1		99 (19)
Positive LOXL2 staining	1.832 (1.063-3.159)	0.029[a]	129 (41)
Multivariable			
Positive LOXL2 staining	1.830 (1.032-3.244)	0.039[a]	
Sex	0.663 (0.383-1.149)	0.143	
Age	1.626 (0.963-2.747)	0.069	
TNM stage	0.494 (0.246-0.991)	0.047[a]	
T stage	1.417 (0.945-2.125)	0.092	
N stage	1.729 (1.080-2.769)	0.023[a]	
M stage	10.822 (3.419-34.249)	<0.0001[a]	
Grade	1.021 (0.496-2.104)	0.954	

Multivariable analysis was adjusted for age, sex, TNM stage, N stages, M stages and grade of differentiation. CI, confidence interval; HR, hazard ratio; LOXL2, lysyl oxidase-like 2; OS, survival analysis; TNM, tumor-node metastasis. [a]P<0.05.

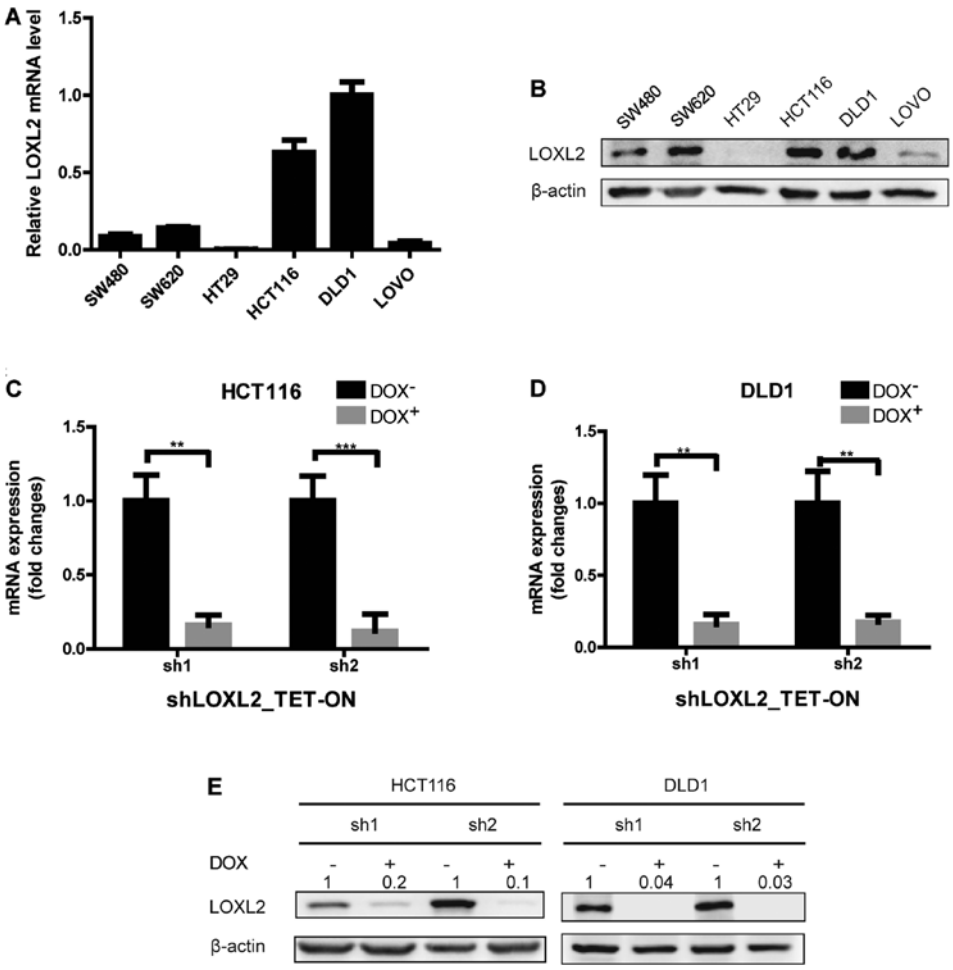

Figure 2. Expression of LOXL2 in CRC cell lines. (A) RT-qPCR analysis of LOXL2 mRNA levels in 6 CRC cell lines. ACTB mRNA was used as an internal control. (B) Western blot analysis of the level of LOXL2 protein in 6 CRC cell lines. β-actin was used as a loading control. RT-qPCR analysis of LOXL2 expression level in (C) HCT116 and (D) DLD1 cells that were transduced with a shLOXL2 TET-ON virus in the absence and presence of DOX. **P<0.01, ***P<0.001. (E) Representative western blots of LOXL2 protein level in the shLOXL2 TET-ON HCT116 and DLD1 cells in the absence and presence of DOX. RT-qPCR, reverse transcription-quantitative polymerase chain reaction; LOXL2, Lysyl oxidase-like 2; CRC, colorectal cancer; DOX, doxycycline; sh, short hairpin RNA.

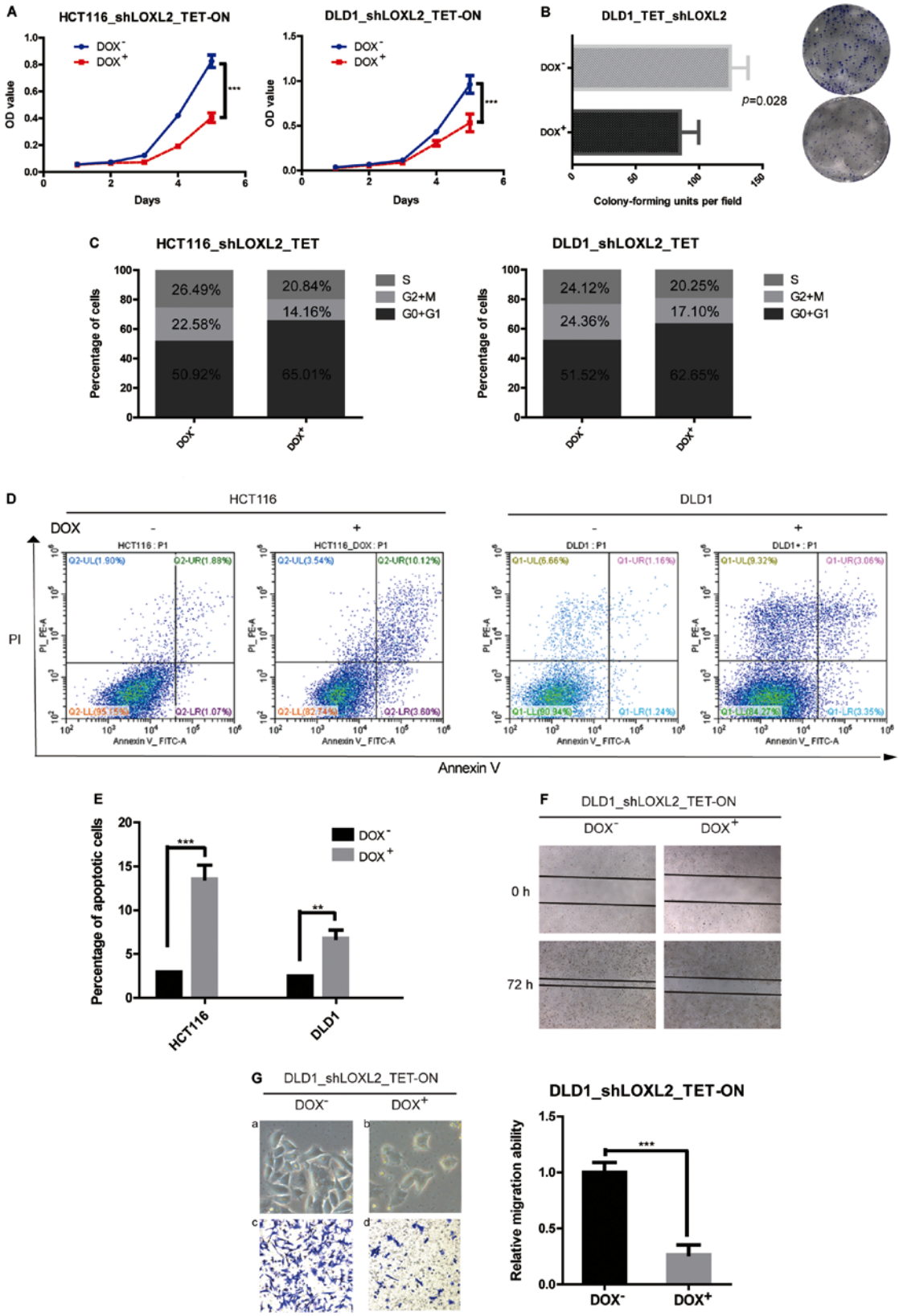

Figure 3. Effect of LOXL2 knockdown in CRC cells *in vitro*. (A) The proliferation of shLOXL2 TET-ON-transduced HCT116 and DLD1 cells in the absence and presence of DOX was analyzed by a Cell Counting Kit-8 assay. The cell numbers were analyzed every day for 5 days. ***P<0.001. (B) Colony-forming assay in shLOXL2 TET-ON-transduced DLD1 cells. Representative images are shown on the right. (C) The percentage of cells in each phase of cell cycle as determined by flow cytometric analysis of shLOXL2 TET-ON-transduced HCT116 and DLD1 cells. (D) Results from flow cytometry apoptosis assay in shLOXL2 TET-ON-transduced HCT116 and DLD1 cells. (E) The proportion of apoptotic cells as determined by flow cytometry in shLOXL2 TET-ON-transduced HCT116 and DLD1 cells. **P<0.01, ***P<0.001. (F) The migratory capacity of shLOXL2 TET-ON-transduced DLD1 cells was determined by a wound-healing assay. The extent of migration was determined at 48 h after the initial scratch wound. Magnification, x40. (G) (a and b) Representative phase-contrast images of shLOXL2 TET-ON-transduced DLD1 cells. Magnification, x200. (c and d) Transwell migration assay for shLOXL2 TET-ON-transduced DLD1 cells. The relative migratory ability was normalized to the migratory ability of the cells that were treated without doxycycline. ***P<0.001. LOXL2, Lysyl oxidase-like 2; sh, short hairpin RNA.

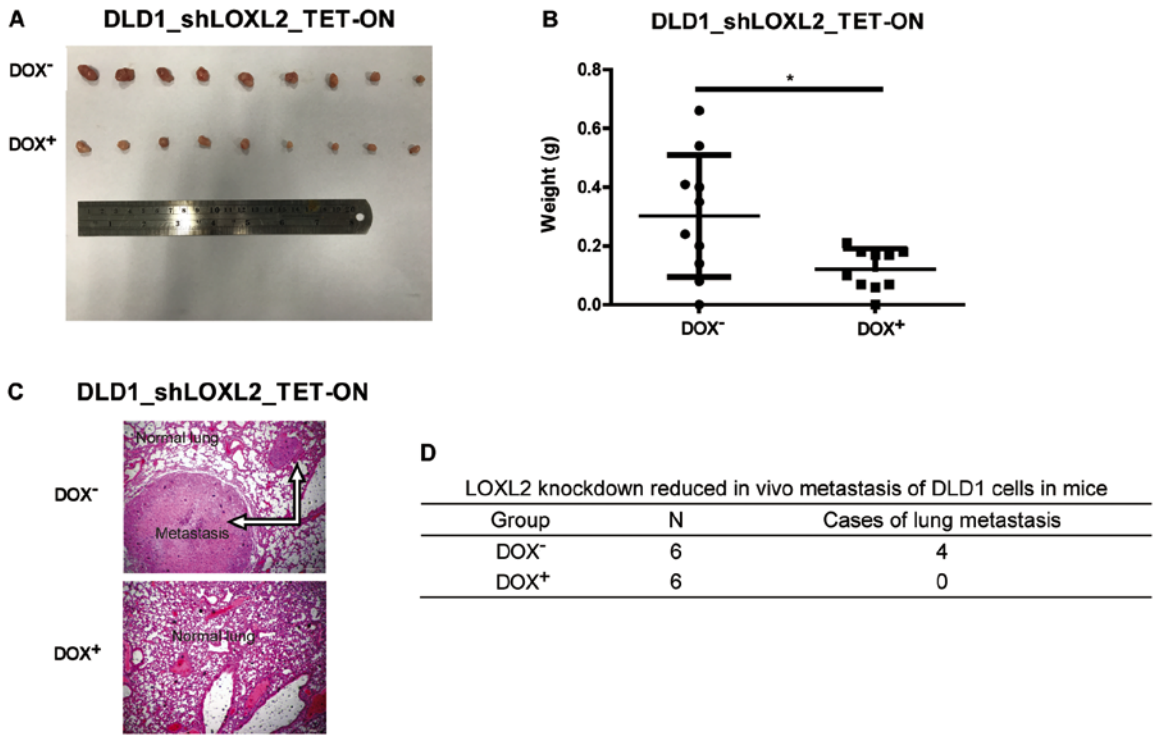

D

LOXL2 knockdown reduced in vivo metastasis of DLD1 cells in mice

Group	N	Cases of lung metastasis
DOX$^-$	6	4
DOX$^+$	6	0

Figure 4. Knockdown of LOXL2 inhibits tumor growth and metastasis in colorectal cancer *in vivo*. ShLOXL2 TET-ON-transduced DLD1 cells were inoculated into mice to generate a xenograft tumor model. The mice were randomized into two groups (5 mice/group): DOX$^-$ and DOX$^+$. The mice were treated every other day with normal water (control group) or water with DOX (treatment group) for 4 weeks. (A) Images of tumors from both groups after 4 weeks of treatment. (B) The weight of the tumors in the two groups after 4 weeks of treatment. (C) shLOXL2 TET-ON-transduced DLD1 cells were injected into the tail vein of nude mice. Images of lung metastases as indicated by the hematoxylin and eosin-stained sections. (D) The incidence of lung metastases in each group. n=6 for each group. Magnification, x50. DOX, doxycycline; LOXL2, Lysyl oxidase-like 2.

of CRC cells *in vitro* (HCT116, P<0.0001; DLD1, P=0.0002) (Fig. 3A). A similar pattern was observed in the colony-forming assays, in which the knockdown of LOXL2 significantly decreased the clonogenicity of DLD1 cells compared with the cells without DOX (85.00±8.505 vs. 124.7± 8.110, respectively; P=0.0279) (Fig. 3B).

LOXL2 knockdown induces cell cycle arrest and apoptosis in CRC cells. To investigate the mechanism for the anti-proliferative effect of the knockdown of LOXL2 in CRC cells, the cell cycle distribution was analyzed using flow cytometry. The silencing of LOXL2 in HCT116 and DLD1 cells resulted in an increase in cells in the G_0/G_1 phase with a decrease in the proportion of S-phase cells compared with the control cells (Fig. 3C). The data showed that the depletion of LOXL2 decreased cell proliferation by cell cycle arrest. The effects of LOXL2 silencing on apoptotic cell death were also examined. Flow cytometry analysis showed that while only 3.0% of HCT116 and 2.5% of DLD1 cells in the absence of DOX were Annexin V-positive, ~13.6% of HCT116 and 6.8% of DLD1 cells with silenced LOXL2 exhibited Annexin V-positive staining (Fig. 3D and E). These results suggested that LOXL2 might be involved in the inhibition of apoptosis.

LOXL2 knockdown impairs the migration of CRC cells and induces mesenchymal-epithelial transition in vitro. As the overexpression of LOXL2 in the clinical data analysis was associated with distant metastasis, wound-healing and Transwell assays were performed to assess the effect of LOXL2 knockdown on the migratory ability of CRC cells. Wound closure rates and cell migration were decreased after LOXL2 knockdown compared with the control group (Fig. 3F and G). Furthermore, LOXL2 knockdown also induced morphological changes in CRC cells, including a loss of cell dispersion, and the formation of intercellular junctions and tight clusters (Fig. 3Ga and b), suggesting a mesenchymal-epithelial transition.

LOXL2 knockdown impairs the growth of tumor xenografts in vivo. The effect of LOXL2 expression on CRC cells was examined *in vivo*. Immunodeficient nude mice were subcutaneously injected with DLD1 cells harboring DOX-inducible LOXL2 shRNA and randomized into two groups. In one group, DOX was administered in the drinking water to induce shRNA expression and LOXL2 knockdown, while normal water was administered in the control group. The growth of the tumor xenografts was monitored over the following 4 weeks. As shown in Fig. 4A, LOXL2 depletion resulted in a marked reduction in tumor size compared with the controls. The tumors from the LOXL2-knockdown group were significantly smaller after 4 weeks compared with tumors from the control group (P=0.0177; Fig. 4B). This finding demonstrated that LOXL2 silencing was able to reduce the growth of CRC cell *in vivo*.

The role of LOXL2 in tumor metastasis was further investigated by injecting DLD1 cells harboring DOX-inducible LOXL2 shRNA into the tail vein of nude mice. The mice were treated every other day with normal water (control) or water

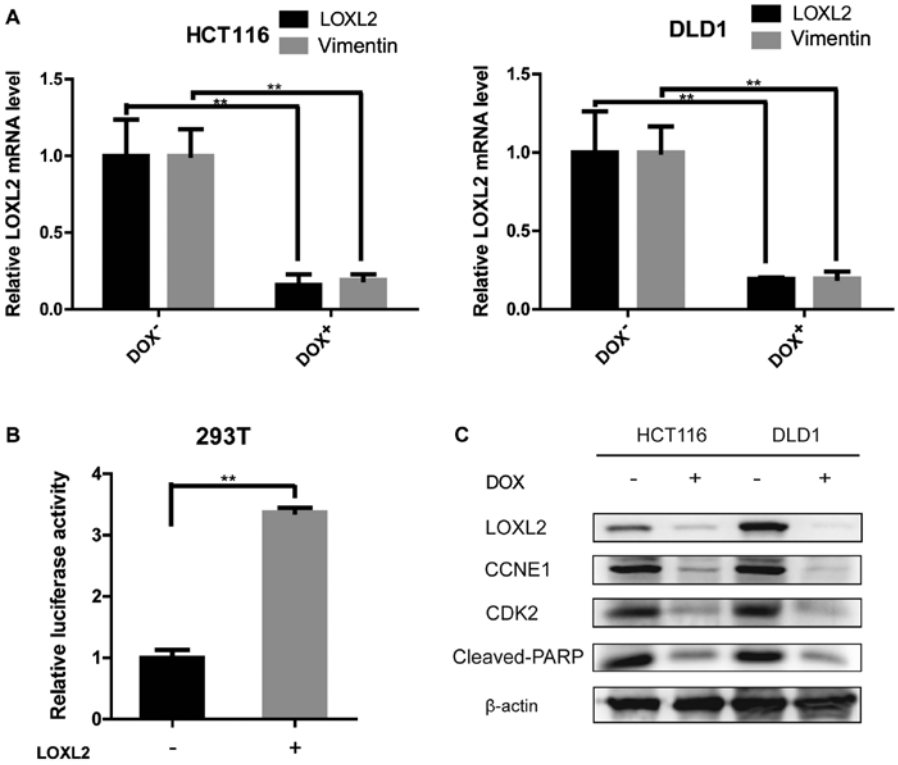

Figure 5. Knockdown of LOXL2 affects the expression of vimentin, cyclin E1 and poly (ADP-ribose) polymerase 1. (A) Quantitative polymerase chain reaction analysis of vimentin expression in shLOXL2 TET-OFF and TET-ON-transduced HCT116 and DLD1 cells. ACTB was used as a control. **P<0.01. (B) The overexpression of LOXL2 increased the activity of the vimentin promoter. The vimentin-Luc reporter plasmid was co-transfected with the pGL3 basic plasmid or pGL3-LOXL2 plasmid into 293T cells, along with the *Renilla* luciferase plasmid. Luciferase activity was normalized to *Renilla* levels and expressed as fold changes to the expression of pGL3 basic plasmid. **P<0.01. (C) Western blot analysis of the transcriptional activators of epithelial-mesenchymal transition in shLOXL2 TET-OFF and TET-ON-transduced HCT116 and DLD1 cells. ACTB was used as the loading control. CCNE1, cyclin E1; CDK2, cyclin dependent kinase 2; DOX, doxycycline; LOXL2, lysyl oxidase-like 2.

with DOX (treatment group; 1 mg/ml) for 8 weeks. Compared with the control mice, the mice receiving DOX developed significantly fewer lung metastases (Fig. 4C and D). This finding demonstrated that silencing LOXL2 reduced CRC metastasis *in vivo*.

LOXL2 may regulate the expression of vimentin, cyclin E1 and cleaved-PARP-1. The knockdown of LOXL2 induced morphological changes in CRC cells, which are indicative of mesenchymal-epithelial transition (Fig. 3Ga and b). These results prompted us to examine the effect of LOXL2 knockdown on epithelial-mesenchymal transition (EMT) transcriptional regulators and markers. In the LOXL2 knocked down-HCT116 and DLD1 cells, vimentin expression, as determined by qPCR, was decreased compared with the control cells (Fig. 5A). The protein levels of vimentin in DLD1 and HCT116 cell lines were repeatedly analyzed. Unfortunately, vimentin expression was extremely low in western blots in both cell lines. Previous published studies also confirmed the results of the present study (22). To evaluate the mechanism by which LOXL2 affects the expression of vimentin, luciferase assays were performed using a luciferase reporter driven by the vimentin promoter (Fig. 5B). The transfection of 293T cells with pGL3-LOXL2 was able to significantly increase luciferase activity that was driven by the vimentin promoter, implying that LOXL2 may induce vimentin expression. The levels of the cell cycle regulator, CDK2, and its partner cyclin E were examined. The activity of CDK2 is maximal during S and G_2 phases; CDK2 is activated by interaction with cyclin E during the early stages of DNA synthesis to permit G_1-S transition (23). Decreased levels of CDK2 and cyclin E were demonstrated in LOXL2-knocked down cells compared with the control cells (Fig. 5C). PARP degradation was also detected by western blotting to confirm the ability of LOXL2 to inhibit apoptosis (Fig. 5C). These data may explain why a depletion of LOXL2 reduced cell proliferation and induced apoptosis.

Discussion

The LOX family contributes to fibrotic matrix crosslinking and stabilization by catalyzing the covalent interchain crosslink of collagen in the ECM (24). The role of LOXL2 has been intensively studied in fibrotic diseases. Ikenaga *et al* (8) revealed that the selective targeting of LOXL2 suppressed the progression of hepatic fibrosis. LOXL2 levels are elevated in the heart tissues and serum of patients with heart failure (HF). Additionally, heart dysfunction and a high level of HF biomarkers are associated with high LOXL2 levels. In mice, LOXL2 activation is crucial for myocardial fibrosis and the development of HF. LOXL2 crosslinks with collagen fibers to activate fibroblasts, and activated fibroblasts secrete further collagen as well as LOXL2. Through this positive feedback loop, LOXL2 triggers cardiac interstitial fibrosis and HF (9).

LOXL2 has also been shown to serve an important role in cancer, mostly through its functions in the ECM. LOXL2 is critical for metastatic niche and tumor ECM formation in hepatocellular carcinoma (13). LOXL2 is overexpressed in cancer-associated fibroblasts (CAFs) in colon cancer (12). Targeting LOXL2 with an allosteric antibody was effective in reducing the number of CAFs in xenograft models of cancer (25). LOXL2 expression is associated with metastasis and poor survival in patients with breast cancer (26), and promotes cancer invasion by downregulating the extracellular protein tissue inhibitor of matrix metalloproteinase-9 and -1 (27). Furthermore, LOXL2 has been verified to be associated with the metastasis of colorectal cancer cells *in vitro* through EMT (28).

In the present study, LOXL2 expression was markedly higher in CRC tissues compared with the adjacent noncancerous tissues at both the mRNA and protein level. These results are consistent with previous microarray data by the authors (15). Several studies have shown that LOXL2 functions as a prognostic marker in various types of cancer, including colon cancer (12). Whereas other reports have focused on its role in the ECM, the nuclear localization of LOXL2 in CRC cells was revealed in the present study. It was demonstrated with the retrospective analysis of 228 CRC tissues and normal adjacent colon tissues and clinical data that high intracellular expression levels of LOXL2 were associated with a poor prognosis. In addition, elevated LOXL2 expression was associated with more advanced clinical and pathological features, including TNM staging and distant metastasis. Univariate and multivariate Cox regression hazard analyses showed that LOXL2 might be a valuable independent biomarker for the prognosis of patients with CRC. These findings prompted further study of the molecular mechanisms of LOXL2 in CRC. It was identified that the depletion of LOXL2 by DOX-induced expression of shRNA inhibited the proliferation of CRC cells via cell cycle arrest and apoptosis. Furthermore, the depletion of LOXL2 also impaired the migratory activity of CRC cells *in vitro* and *in vivo*.

EMT has been demonstrated as a key event in cancer metastasis, and plays a key role in driving cancer cells to invade the adjacent normal tissues (29). Two mechanisms have previously been demonstrated for the function of LOXL2 in EMT. Firstly, LOXL2 interacts with Snail1, which results in the repression of CDH1 to induce EMT (30). Secondly, LOXL2 has been implicated in the activation of FAK kinase in a Snail1-independent pathway, which downregulates genes that are associated with epidermal differentiation and cell polarity to promote the mesenchymal phenotype (14). The luciferase assay results in the present study indicated that LOXL2 expression was also able to significantly increase the promoter activity of vimentin, suggesting that LOXL2 may exert its effects by inducing vimentin expression.

In conclusion, it was observed that a high level of LOXL2 mRNA and protein expression in CRC patients was associated with impaired overall survival. The knockdown of LOXL2 *in vitro* and *in vivo* induced cell cycle arrest and apoptosis. However, a phase II study previously indicated that the outcomes in patients with metastatic CRC and KRAS mutation were not improved following the addition of simtuzumab (a monoclonal antibody to LOXL2) (31). The results of the present study provide novel insights into the biology of CRC cells and suggest that LOXL2 may be a potential target for tumor therapy.

Acknowledgements

Not applicable.

Funding

The present study was funded by the National High Technology Research and Development Program of China (863 Program; grant no. SQ2014SFOZD00314) and the National Natural Science Foundation of China (grant nos. 81372636, 81572378 and 81302089).

Availability of data and materials

The datasets used and/or analyzed during the current study are available from the corresponding author on reasonable request.

Authors' contributions

XC conducted most of the molecular and animal experiments, and was a major contributor in writing the manuscript. GW analyzed the patient data. WS made substantial contributions to conception and design. ZH and HH performed substantial parts of the molecular experiments. LC made substantial contributions to conception and design, and was a major contributor in revising manuscript critically for important intellectual content. All authors read and approved the final manuscript.

Ethics approval and consent to participate

Approval for experiments was obtained from the institutional ethics committee. All applicable international, national, and/or institutional guidelines for the care and use of animals were followed.

Consent for publication

The patient, or their parent, guardian or next of kin provided written informed consent for the publication of any associated data and accompanying images.

Competing interests

The authors declare that they have no competing interests.

References

1. International Agency for Research on Cancer: Population Fact Sheets: World. http://gco.iarc.fr/today/fact-sheets-populations?population=900&sex=0. Accessed July 25, 2017.
2. Siegel R, DeSantis C, Virgo K, Stein K, Mariotto A, Smith T, Cooper D, Gansler T, Lerro C, Fedewa S, *et al*: Cancer treatment and survivorship statistics, 2012. CA Cancer J Clin 62: 220-241, 2012.
3. Sankaranarayanan R, Swaminathan R, Brenner H, Chen K, Chia KS, Chen JG, Law SC, Ahn YO, Xiang YB, Yeole BB, *et al*: Cancer survival in Africa, Asia, and Central America: A population-based study. Lancet Oncol 11: 165-173, 2010.

4. Heald RJ and Ryall RD: Recurrence and survival after total mesorectal excision for rectal cancer. Lancet 1: 1479-1482, 1986.
5. van Gijn W, Marijnen CAM, Nagtegaal ID, Kranenbarg EM, Putter H, Wiggers T, Rutten HJ, Påhlman L, Glimelius B and van de Velde CJ; Dutch Colorectal Cancer Group: Preoperative radiotherapy combined with total mesorectal excision for resectable rectal cancer: 12-year follow-up of the multicentre, randomised controlled TME trial. Lancet Oncol 12: 575-582, 2011.
6. Polónia A, Coimbra M, Reis S, Tavares A, Raimundo A, Santos LL, Jeronimo C and Henrique RM: Expression of histone modifying enzymes and histone post-translational marks in colorectal cancer. Virchows Arch 463: 125, 2013.
7. Barker HE, Cox TR and Erler JT: The rationale for targeting the LOX family in cancer. Nat Rev Cancer 12: 540-552, 2012.
8. Ikenaga N, Peng ZW, Vaid KA, Liu SB, Yoshida S, Sverdlov DY, Mikels-Vigdal A, Smith V, Schuppan D and Popov YV: Selective targeting of lysyl oxidase-like 2 (LOXL2) suppresses hepatic fibrosis progression and accelerates its reversal. Gut 66: 1697-1708, 2017.
9. Yang J, Savvatis K, Kang JS, Fan P, Zhong H, Schwartz K, Barry V, Mikels-Vigdal A, Karpinski S, Kornyeyev D, *et al*: Targeting LOXL2 for cardiac interstitial fibrosis and heart failure treatment. Nat Commun 7: 13710, 2016.
10. Wu L and Zhu Y: The function and mechanisms of action of LOXL2 in cancer (Review). Int J Mol Med 36: 1200-1204, 2015.
11. Park JS, Lee JH, Lee YS, Kim JK, Dong SM and Yoon DS: Emerging role of LOXL2 in the promotion of pancreas cancer metastasis. Oncotarget 7: 42539-42552, 2016.
12. Torres S, Garcia-Palmero I, Herrera M, Bartolomé RA, Peña C, Fernandez-Aceñero MJ, Padilla G, Peláez-García A, Lopez-Lucendo M, Rodriguez-Merlo R, *et al*: LOXL2 is highly expressed in cancer-associated fibroblasts and associates to poor colon cancer survival. Clin Cancer Res 21: 4892-4902, 2015.
13. Wong CC, Tse AP, Huang YP, Zhu YT, Chiu DK, Lai RK, Au SL, Kai AK, Lee JM, Wei LL, *et al*: Lysyl oxidase-like 2 is critical to tumor microenvironment and metastatic niche formation in hepatocellular carcinoma. Hepatology 60: 1645-1658, 2014.
14. Moreno-Bueno G, Salvador F, Martín A, Floristán A, Cuevas EP, Santos V, Montes A, Morales S, Castilla MA, Rojo-Sebastián A, *et al*: Lysyl oxidase-like 2 (LOXL2), a new regulator of cell polarity required for metastatic dissemination of basal-like breast carcinomas. EMBO Mol Med 3: 528-544, 2011.
15. Fu J, Tang W, Du P, Wang G, Chen W, Li J, Zhu Y, Gao J and Cui L: Identifying microRNA-mRNA regulatory network in colorectal cancer by a combination of expression profile and bioinformatics analysis. BMC Syst Biol 6: 68, 2012.
16. Cui X, Liu B, Zheng S, Dong K and Dong R: Genome-wide analysis of DNA methylation in hepatoblastoma tissues. Oncol Lett 12: 1529-1534, 2016.
17. Wang G, Shen W, Liu CY, Liu Y, Wu T, Cui X, Yu T, Zhu Y, Song J, Du P, *et al*: Phosphorylase kinase β affects colorectal cancer cell growth and represents a novel prognostic biomarker. J Cancer Res Clin Oncol 143: 971-980, 2017.
18. Cui X, Yang Y, Jia D, Jing Y, Zhang S, Zheng S, Cui L, Dong R and Dong K: Downregulation of bone morphogenetic protein receptor 2 promotes the development of neuroblastoma. Biochem Biophys Res Commun 483: 609-616, 2017.
19. Wiederschain D, Wee S, Chen L, Loo A, Yang G, Huang A, Chen Y, Caponigro G, Yao YM, Lengauer C, *et al*: Single-vector inducible lentiviral RNAi system for oncology target validation. Cell Cycle 8: 498-504, 2009.
20. Liu CY, Yu T, Huang Y, Cui L and Hong W: ETS (E26 transformation-specific) up-regulation of the transcriptional co-activator TAZ promotes cell migration and metastasis in prostate cancer. J Biol Chem 292: 9420-9430, 2017.
21. Liu Y, Wang G, Yang Y, Mei Z, Liang Z, Cui A, Wu T, Liu CY and Cui L: Increased TEAD4 expression and nuclear localization in colorectal cancer promote epithelial-mesenchymal transition and metastasis in a YAP-independent manner. Oncogene 35: 2789-2800, 2016.
22. Findlay VJ, Wang C, Nogueira LM, Hurst K, Quirk D, Ethier SP, Staveley O'Carroll KF, Watson DK and Camp ER: SNAI2 modulates colorectal cancer 5-fluorouracil sensitivity through miR145 repression. Mol Cancer Ther 13: 2713-2726, 2014.
23. Terret ME, Lefebvre C, Djiane A, Rassinier P, Moreau J, Maro B and Verlhac MH: DOC1R: A MAP kinase substrate that control microtubule organization of metaphase II mouse oocytes. Development 130: 5169-5177, 2003.
24. Liu SB, Ikenaga N, Peng ZW, Sverdlov DY, Greenstein A, Smith V, Schuppan D and Popov Y: Lysyl oxidase activity contributes to collagen stabilization during liver fibrosis progression and limits spontaneous fibrosis reversal in mice. FASEB J 30: 1599-1609, 2016.
25. Barry-Hamilton V, Spangler R, Marshall D, McCauley S, Rodriguez HM, Oyasu M, Mikels A, Vaysberg M, Ghermazien H, Wai C, *et al*: Allosteric inhibition of lysyl oxidase-like-2 impedes the development of a pathologic microenvironment. Nat Med 16: 1009-1017, 2010.
26. Barker HE, Chang J, Cox TR, Lang G, Bird D, Nicolau M, Evans HR, Gartland A and Erler JT: LOXL2-mediated matrix remodeling in metastasis and mammary gland involution. Cancer Res 71: 1561-1572, 2011.
27. Kouhkan F, Motovali-Bashi M and Hojati Z: The influence of interstitial collagenase-1 genotype polymorphism on colorectal cancer risk in Iranian population. Cancer Invest 26: 836-842, 2008.
28. Park PG, Jo SJ, Kim MJ, Kim HJ, Lee JH, Park CK, Kim H, Lee KY, Kim H, Park JH, *et al*: Role of LOXL2 in the epithelial-mesenchymal transition and colorectal cancer metastasis. Oncotarget 8: 80325-80335, 2017.
29. Thiery JP, Acloque H, Huang RY and Nieto MA: Epithelial-mesenchymal transitions in development and disease. Cell 139: 871-890, 2009.
30. Peinado H, Del Carmen Iglesias-de la Cruz M, Olmeda D, Csiszar K, Fong KS, Vega S, Nieto MA, Cano A and Portillo F: A molecular role for lysyl oxidase-like 2 enzyme in snail regulation and tumor progression. EMBO J 24: 3446-3458, 2005.
31. Hecht JR, Benson AB III, Vyushkov D, Yang Y, Bendell J and Verma U: A phase II, randomized, double-blind, placebo-controlled study of simtuzumab in combination with FOLFIRI for the second-line treatment of metastatic KRAS mutant colorectal adenocarcinoma. Oncologist 22: 243-e23, 2017.